

EGG-SCM--8069

DE91 001826

CERAMIC JOINT INTERFACE DIAGNOSTICS
WITH ULTRASONIC REFLECTION SIGNAL ENERGIES

K. L. Telschow and J. B. Walter

Published June 1988

Idaho National Engineering Laboratory
EG&G Idaho Inc.
Idaho Falls, ID 83415-2209

Prepared for the
Interior Department's Bureau of Mines
Under Contract No. J0134035
Through the
U.S. Department of Energy
Idaho Operations Office
Contract No. DE-AC07-ID01570

MASTER

DISTRIBUTION OF THIS DOCUMENT IS UNLIMITED

422

ABSTRACT

The properties of silicon nitride ceramic joints, prepared by hot isostatic pressing, have been investigated by recording the reflected ultrasonic elastic wave off the joint interface. Experimental and theoretical analysis of the reflected signal energy has shown that properties of the joint interface such as thickness, joining compound composition, inclusions, and voids, can be imaged over the joint plane. A model incorporating plane waves shows that the reflected signal energy is a function of joint thickness, joint/host acoustic impedance and transducer bandwidth. For joint thicknesses less than the average ultrasonic wavelength in the joint, the reflected signal energy depends quadratically on the thickness. This dependence was verified by for several joints by direct measurement. In the opposite regime, where the joint thickness is greater than the ultrasonic wavelength, the reflected signal energy is independent of thickness and only a function of the joint/host acoustic impedance mismatch. This regime was not accessible with the joints available for this work. These results are valid for wide bandwidth transducers. The results suggest that for a given range of thicknesses, measurement of the joint energy with broadband transducers with different center frequencies could provide a means of determining both the joint thickness and joint/host acoustic impedance mismatch. Joint thickness is the most prominent parameter that can be probed with ultrasonics and its effect on fracture toughness should be an important parameter in determining the quality of joints. Qualitatively, the reflected signal energy method of data analysis is a rapid means for assessing joint quality with respect to thickness, inclusions, and voids.

CONTENTS

ABSTRACT	ii
INTRODUCTION	1
JOINT REFLECTION SIGNAL ENERGY MODEL DEVELOPMENT	3
Theory	3
Experiment	7
CERAMIC HIPPED JOINTS - INCLUSIONS AND VOIDS	13
Microfocus X-ray Experiment	13
Ultrasonic C-scans	14
CERAMIC HIPPED JOINTS - FRACTURE TESTS	18
Vee Cuts	18
Modulus of Rupture Bars	20
CONCLUSIONS	22
REFERENCES	23
APPENDIX A--DERIVATION OF THE JOINT REFLECTION SIGNAL ENERGY: PLANE WAVE ANALYSIS	25

FIGURES

1. Plane wave joint interface reflection signal model diagram.....	4
2. Dependence of the calculated reflected energy on the joint interface thickness for a glass joint and a water-filled joint...	5
3. Sensitivity of the reflected energy to the acoustic impedance of the joint interface as a function of joint thickness	5
4. Dependence of the reflected energy on the acoustic impedance mismatch of the joint	6
5. Dependence of the reflected signal energy on joint thickness for three broadband transducers with center frequencies of 10, 25, and 50 MHz.....	6
6. Joint interface reflection signal in the time domain for the joint #37MRCR1A.....	8

7. C-scan of #37MRCR1A joint plane reflected signal energies. The in-plane separation between measurements is 1 mm.....	9
8. Micrographs of the joint interface for #37MRCR1A along the central section.....	10
9. Normalized joint reflection energies versus measured joint thicknesses at the same location for nine different joints processed under a variety of external parameters.....	11
10. C-scan of the joint reflection signal energy from 29(KY/126) joint, performed with an 80 MHz, (75 μ m wavelength) 0.125-in. (3.2-mm) transducer.	15
11. C-scan of the joint reflection signal energy from 29(KY/1) joint, performed with an 80 MHz, (75 μ m wavelength) 0.125-in. (3.2-mm) transducer.....	16
12. Micrograph of the detected flaw in joint 29(KY/126).....	17
13. Plot of the joint reflection signal energies obtained by scanning before fracture testing for a HIPped Kyon/glass/Kyon joint 25(Ky/1).....	19
14. Plot of the joint reflection signal energies obtained by scanning before fracture testing for a HIPped NC/glass/NC joint 20(NC/1).....	21

CERAMIC JOINT INTERFACE DIAGNOSTICS
WITH ULTRASONIC REFLECTION SIGNAL ENERGIES

INTRODUCTION

Joining of ceramic materials with strong joints is critical for producing large structures, such as heat engines, and composite parts with mechanical properties appropriate for the intended application. Because the integrity of the resulting bonds is most important, a nondestructive means of determining joint characteristics would be valuable for determining acceptable joints and extending service lifetimes. The goal of this task, therefore, was to evaluate, through nondestructive ultrasonic measurements, the integrity of ceramic joints prepared by brazing with a glass joining compound.

This work utilizes silicon nitride ceramic materials joined by a high nitrogen content glass layer through the application of the hot isostatic press (HIP) process as part of the Strategic and Critical Materials Program at the INEL.^{1,2} The ceramic materials were obtained from several suppliers^a and joined by personnel in the Ceramics group at the INEL.² The joined pieces were ultrasonically scanned for joint interface reflection signals and then sectioned for fracture toughness measurements and metallographic analysis.

This report describes the ceramic joint characterization work conducted at the INEL. A variety of joints prepared under different conditions is compared, and conclusions are drawn as to the applicability of ultrasonic measurements to assessing joint characteristics.

a. Kennametal, Inc., Raleigh, NC, supplied the Kyon 2000 for samples 29(KY/126), 29(KY/1), 25(KY/1); Norton Co., Worcester, MA, supplied the NC-132 for sample 20(NC/1); and Ceradyne, Inc., Santa Anna, CA, supplied the Ceralloy 147Y-2 for sample 37MRCRIA.

Ultrasonic signals produced by high frequency transducers were reflected off the joint interface. The signals were processed to produce a C-scan, which is an image of the joint plane illustrating the energies of reflected signals resulting from properties of the joint such as thickness, composition of the joining material, and the presence of voids, cracks, or crystallization of the glass in the joint plane. Joint thickness was accurately measured, allowing good correlation to be found between joint reflection signal energy and joint thickness. This provided a means to calibrate the reflection signals for thickness dependence.

A calculation was performed of the reflection signal energy from a good joint, based on a continuum model, which accounts for acoustic impedance discontinuities at the joint, the joint thickness, and also the finite bandwidth of the incident signal. The model was set up to closely follow the actual experimental conditions of the C-scan joint mapping. The calculation results point out the dependence of the joint's reflected signal energy on the joint thickness and bonding material composition. It was found that for joint thicknesses less than the ultrasonic wavelength in the joint, the reflected signal energy depends quadratically on the joint thickness and is proportional to a parameter describing the joint/host acoustic impedance mismatch. All of the work reported is for thin joints in this regime. The model also indicates that for joint thicknesses greater than the ultrasonic wavelength the signal energy is independent of joint thickness and dependent only on the acoustic impedance of the joint. In this regime a change in signal energy indicates a region of debonding, micro-cracking or voids, independent of the joint thickness. Qualitatively, for both regimes, the reflected signal energy method of data analysis is a rapid means for assessing joint quality with respect to inclusions and voids.

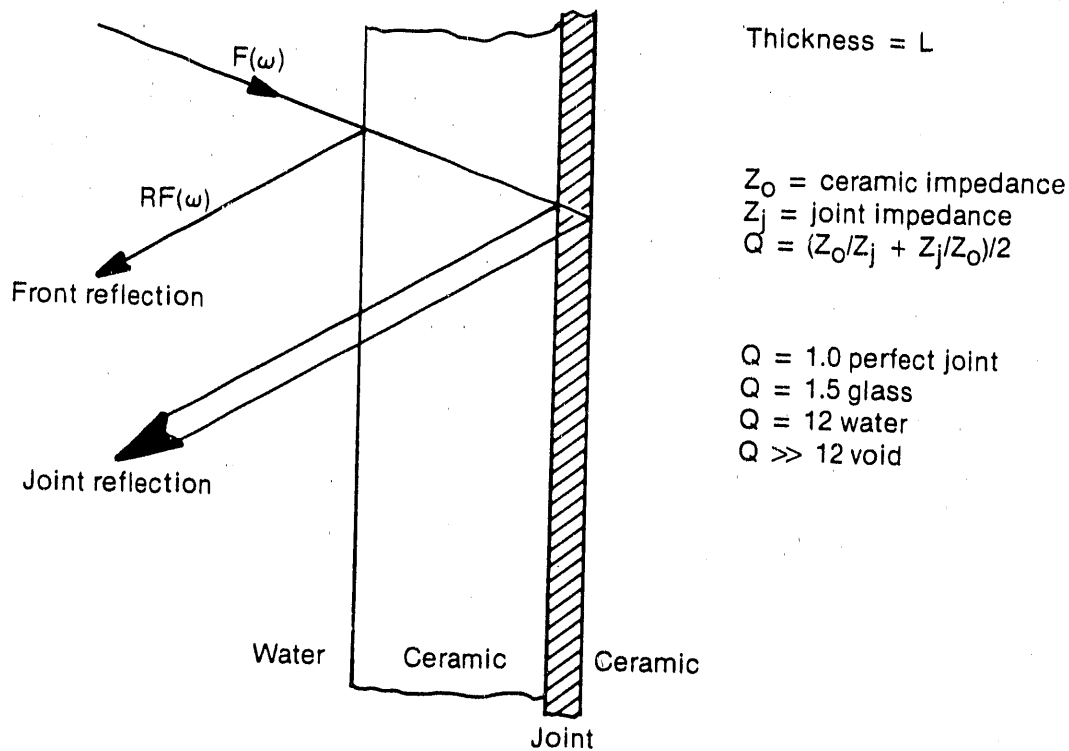
With the analytic model for the joint reflection signal energy as a guide, several joints were scanned, as described below, for both joint analysis and model confirmation.

JOINT REFLECTION SIGNAL ENERGY MODEL DEVELOPMENT

Theory

Calculations of the acoustic energy reflected from a joint were made based on a continuum model. This model was used to identify the joint thickness and acoustic impedance as measurable parameters and to determine the experimental conditions required to measure these parameters. The model is for a joint of finite thickness that is impinged upon by a plane wave acoustic pulse of finite bandwidth. Figure 1 shows a schematic of the joint interface and the relevant reflected signals. The energy reflected from the interface was calculated based on the plane wave reflection coefficients from the joint and the impedance mismatch factor between the host and joint material, Q , which is a function of the ratio of the known impedances of the two materials (see Figure 1 and Appendix A).

This calculation takes into account the interference between reflections from both joint interfaces and the finite bandwidth of the impinging longitudinal wave. The integral for the joint reflection signal energy calculation was evaluated numerically, approximating the incident wave bandwidth as Gaussian. The calculations were made for center frequencies of 10, 25, and 50 MHz and average ultrasonic wavelengths of 600, 240 and 120 μm in the joint material, which approximate the transducers used. Figure 2 shows the calculated energy as a function of the joint thickness for two values of the joint impedance. Above $\sim 25 \mu\text{m}$ thickness, the reflected energy is predicted to show no thickness-dependent variation and to provide a clear measure of the joint's impedance. Below 25 μm , the reflected signal depends strongly on both the thickness and the impedance of the joint. Figure 3 shows the ratio of the two curves in Figure 2 and indicates the maximum contrast ratio that would be seen between regions of good joining (glass joint) and regions of complete debonding (filled with water). It is seen that the reflected energy is most sensitive to impedance changes in thin joints. Figure 4 shows the dependence on the joint impedance for three values of joint thickness. The reflected energy depends nonlinearly on Q and is, in fact, most sensitive for small values of Q for which the impedances are nearly



Incident signal, $F(\omega)$, reflects from the front surface, $RF(\omega)$ and the joint.
 The joint signal energy is calculated as follows:

$$JE = \left(\frac{1-R^2}{R}\right)^2 \left(\frac{Q^2-1}{Q^2}\right) \int |F(\omega)|^2 \frac{Q^2 d\omega}{Q^2 + \cot^2\left(\frac{\omega L}{V}\right)}$$

V = Longitudinal wave velocity in the joint.

8-4487

Figure 1. Plane wave joint interface reflection signal model diagram.

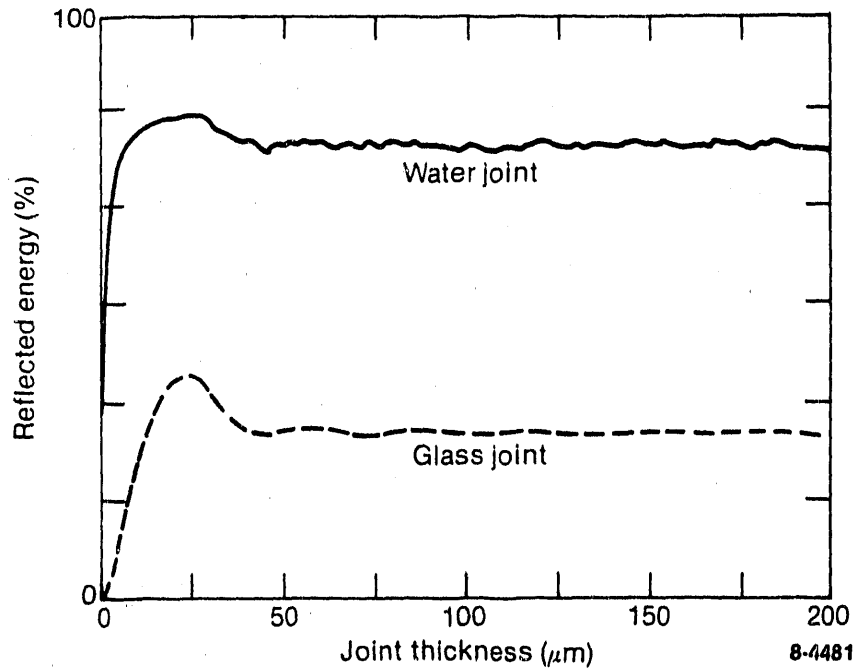


Figure 2. Dependence of the calculated reflected energy on the joint interface thickness for a glass joint and a water-filled joint ($Q = 1.5$ and $12.$). Calculations made for a broadband 50 MHz ($120 \mu\text{m}$) transducer.

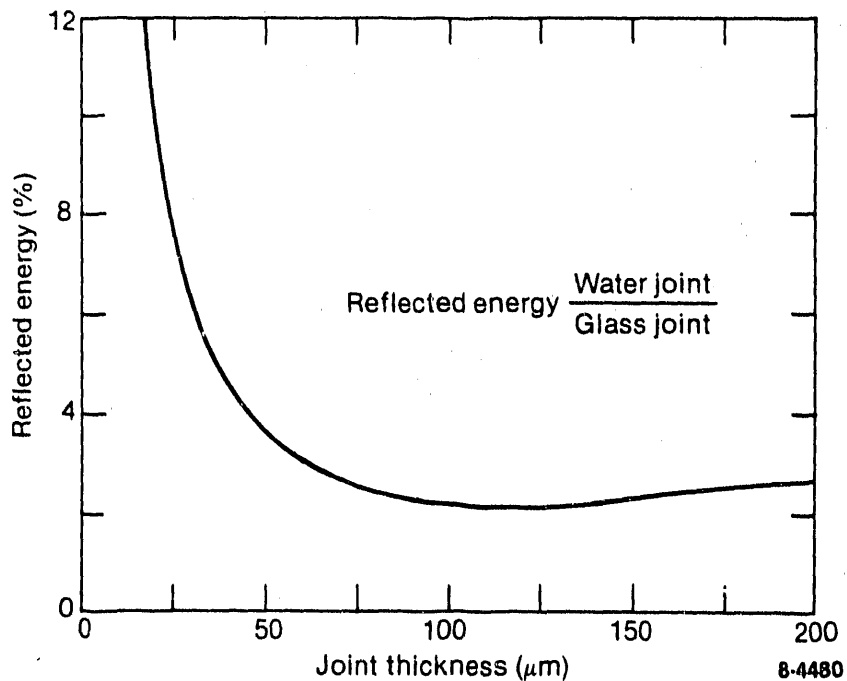


Figure 3. Sensitivity of the reflected energy to the acoustic impedance of the joint interface as a function of joint thickness. Same transducer as for Figure 2.

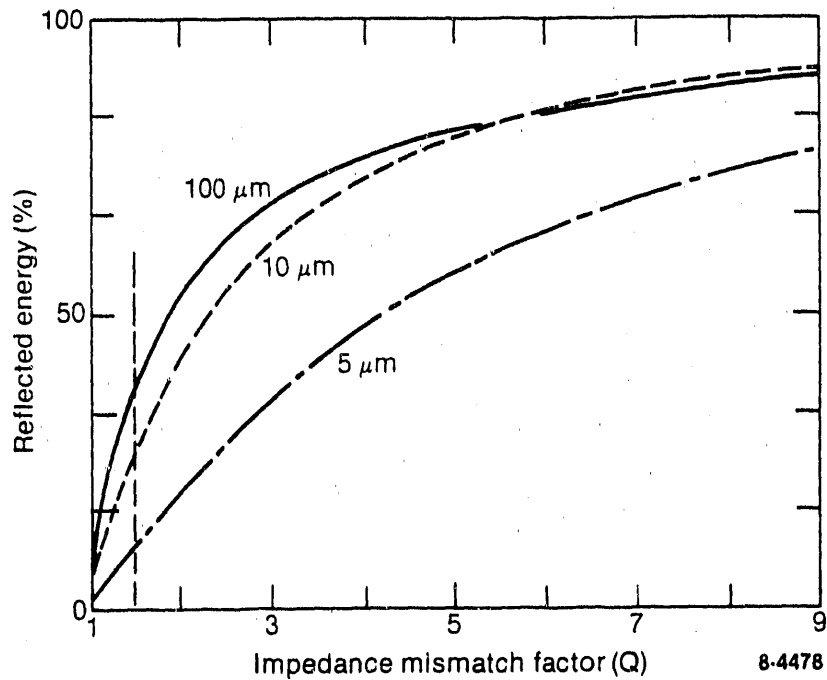


Figure 4. Dependence of the reflected energy on the acoustic impedance mismatch of the joint. Calculations for same transducer as Figure 2. The dashed line is drawn at $Q = 1.5$ which represents a glass filled joint.

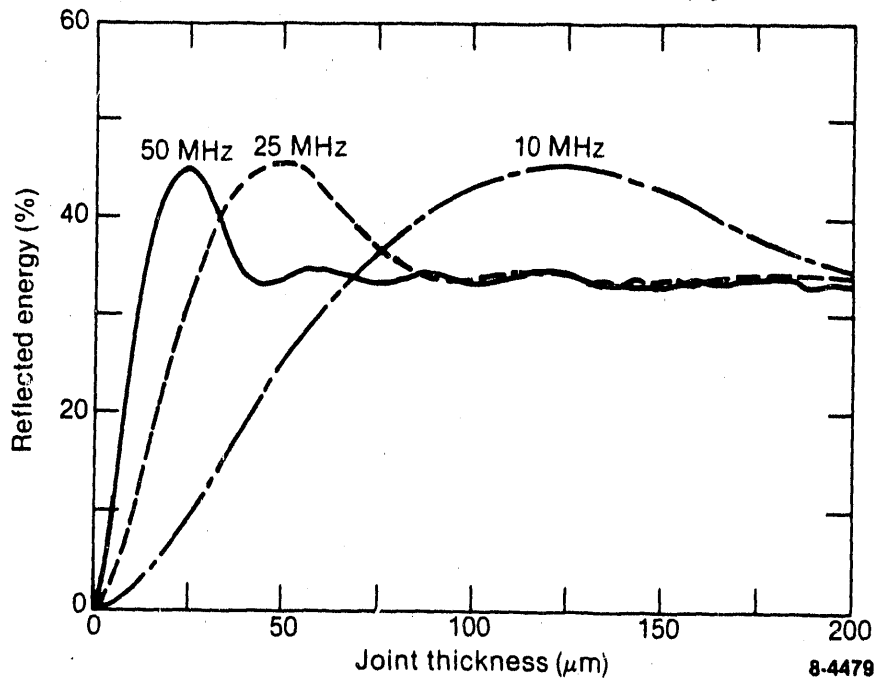


Figure 5. Dependence of the reflected signal energy on joint thickness for three broadband transducers with center frequencies of 10, 25, and 50 MHz (wavelengths of 600, 240 and 120 μm). Calculations are for a glass filled joint ($Q = 1.5$).

matched. Figure 5 shows the reflected energy's dependence on the center frequency of the transducer. The reflected energy peaks at larger values of the joint thickness for lower frequency transducers.

The reflected signal energy curve can be understood by considering the signal energy that would be obtained for a single frequency continuous wave. In this case, there would be interference between waves reflected from the two joint interfaces and a resultant series of zeros in the reflection coefficient periodically spaced at frequencies corresponding to the joint thickness being equal to integral values of half the wavelength. For joint thicknesses greater than the ultrasonic wavelength, the reflected energy's independence of thickness (seen in Figure 5) comes from the wide bandwidth character of the incident waveform. By using a wide bandwidth signal, the energy measurement effectively averages the wavelength (thickness) dependence out of the reflected energy value. This results in the measurement being sensitive only to the ceramic host/joint compound impedance ratio, as stated above. There are then two distinct regions for the joint reflection signal energy: (a) for thicknesses smaller than the wavelength, the energy is proportional to $[(Q^2 - 1)/Q^2](l^2/\lambda^2)$, and can be used to probe both thickness and impedance, and (b) for thicknesses greater than the wavelength, the energy is proportional to $(Q^2 - 1)/Q^2$ and independent of the thickness (see Appendix A).

Experiment

Confirmation of the theoretical model requires knowledge of all the relevant parameters for a given joint; a fact not easily accomplished with HIPped joints because the process leads to a wide variability in results. Success was achieved with a joint prepared with ceramic blocks, 19 x 19 x 24 mm, joined along the smaller dimension. This joint (#37MRCR1A) resulted in a wedge-shaped joint interface, with thicknesses ranging from 24 to 50 μm . Upon sectioning, this joint was found to be free of voids and became a standard joint for determining the thickness dependence of the model. Other nonwedged joints, similar to this one, formed a series of approximately ten joints of the same geometry but processed under different conditions during HIPping. All were scanned with a 20 MHz 0.25-in. (6.35-mm) flat immersion transducer. A typical joint interface

reflection signal (A-scan) is shown in Figure 6. This signal was digitized and its energy calculated numerically for each location in the joint plane. Figure 7 shows a C-scan of the joint signal energies and delineates the wedged thickness. Data throughout the joint plane were obtained by sectioning the joint into squares as shown in Figure 7 and optically measuring the joint thickness. Figure 8 shows the joint cross sections found. These thickness values were then correlated with averages of the C-scan data taken throughout the corresponding squares in order to complete the signal energy versus thickness correlation as shown in Figure 9.

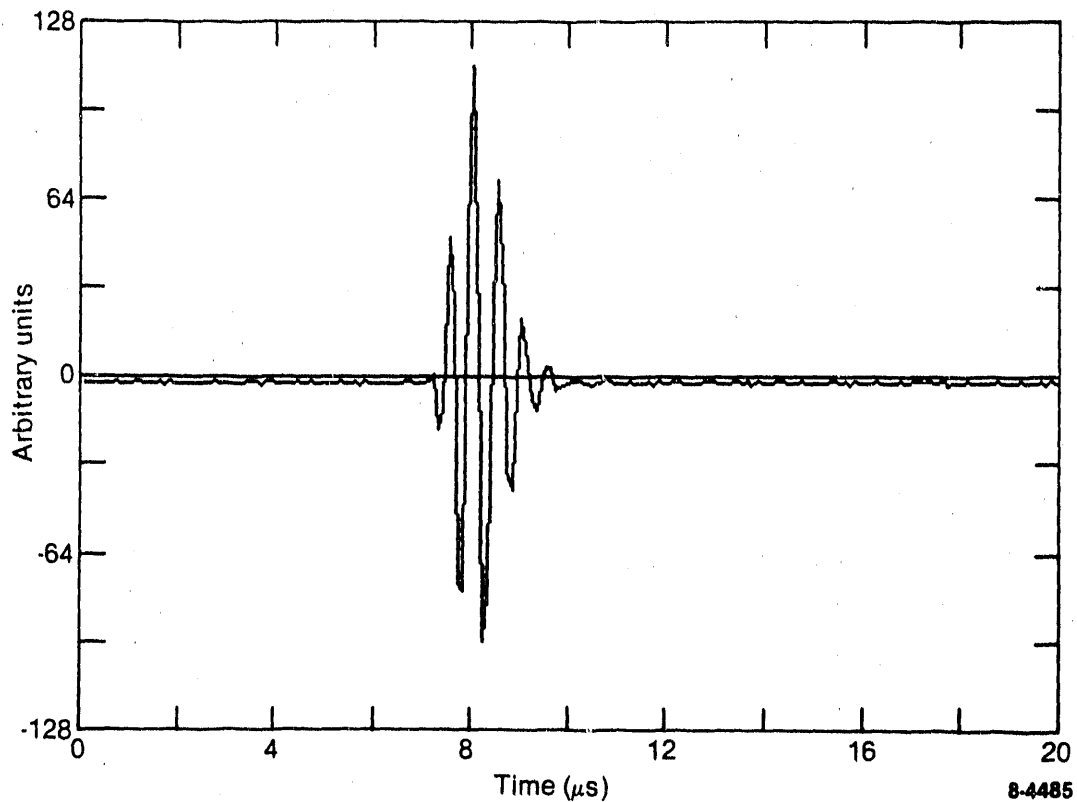


Figure 6. Joint interface reflection signal in the time domain for the joint #37MRCR1A. The incident wave was produced by a 20 MHz, flat faced, 0.25-in. (6.35-mm) aperture transducer in water, with a $240 \mu\text{m}$ wavelength in the joint material.

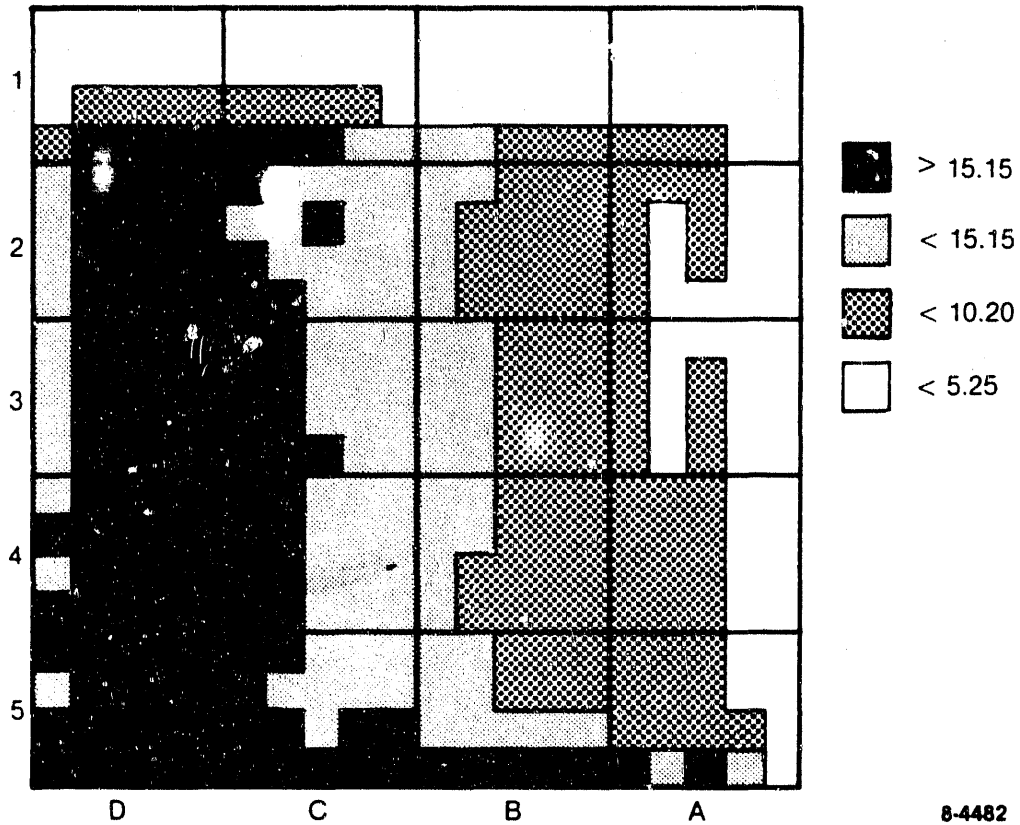


Figure 7. C-scan of #37MRCR1A joint plane reflected signal energies. The in-plane separation between measurements is 1 mm. The sectioning grid used for the thickness and fracture toughness measurements is also shown.



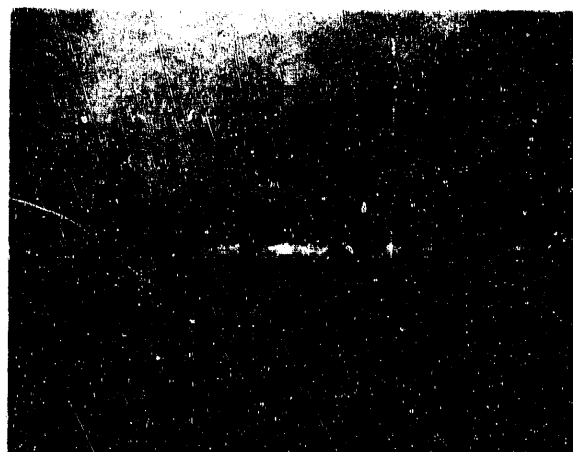
A3



B3



C3



D3

Figure 8. Micrographs of the joint interface for #37MRCR1A along the central section. (50X)

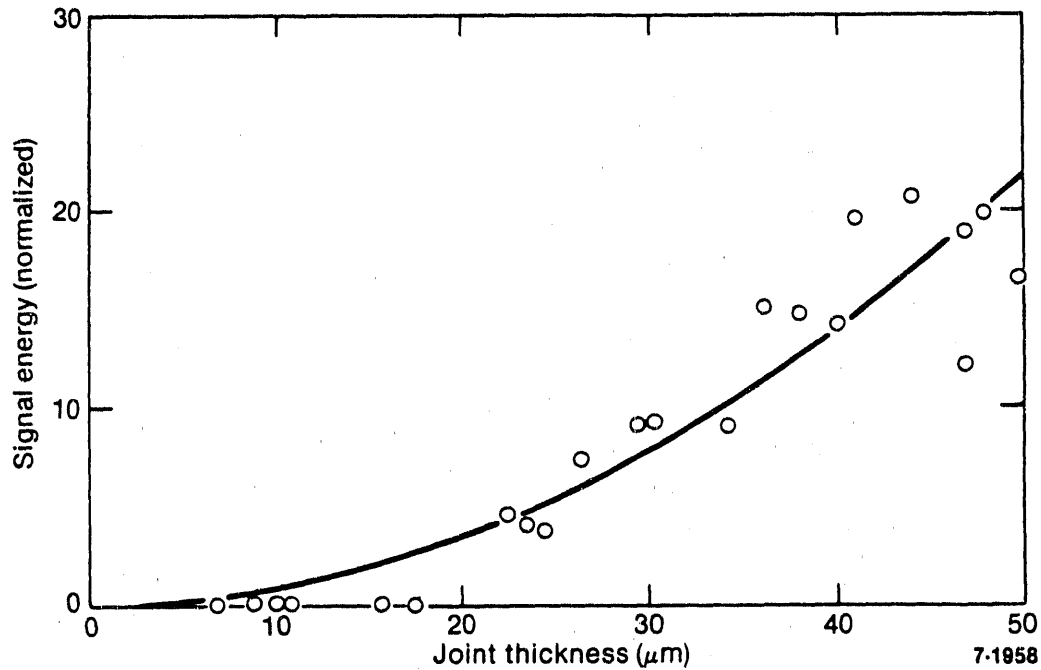


Figure 9. Normalized joint reflection energies versus measured joint thicknesses at the same location for nine different joints processed under a variety of external parameters.

Figure 9 shows the measured joint reflection signal energy as a function of joint thickness for those regions, in several joints, where reliable thickness estimates could be obtained. Most of the joints exhibited significant thickness variations across the joint plane, which account to some extent for the scatter observed. The energy reflected from the interface was calculated based on the reflection coefficients from the joint and the impedance mismatch between the host and joint. The impedances of the host ceramic and glass joining compound were measured from separate bulk samples. The signal energy scales approximately quadratically with joint thickness over the range of thicknesses to 50 μm or greater. This type of behavior is consistent with the calculational model results as indicated in Figure 9 and shows that for these relatively thick joints and for a given glass joining compound, assumed uniformly distributed throughout the joint, thickness is the primary characteristic measured by the ultrasonic reflection signal. The actual measurement is capable of resolving significantly smaller reflected signals (about two orders of magnitude smaller in energy) than shown in Figure 9. Almost all of the stronger joints exhibit reflections in this range that cannot be accounted for by thickness dependence alone. These reflections are possibly due to microcracking near the joint plane or

spreading of the joint region from diffusion of the joining glass into the host ceramic. Most of the joints used in these tests were also subjected to fracture testing and were not available for detailed joint interface analysis. This frustrated the collection of sufficient data to correlate all levels of reflection signal energies observed with known joint characteristics. The data presented here support the thickness dependence of the model and suggest that several other correlations are possible; a more involved series of tests is needed and would be fruitful in establishing this correlation.

CERAMIC HIPPED JOINTS - INCLUSIONS AND VOIDS

Several of the preliminary joints prepared for this program consisted of ceramic blocks approximately 13 x 19 x 5 mm in size joined along the largest face. Due to this small size and thin section, a high frequency transducer (nominal frequency 80 MHz, 75 μ m wavelength) with a 0.125-in. (3.2-mm) aperture was used for the ultrasonic reflection measurements. The ultrasonic scans proved to be very useful for qualitative tests of joint integrity, providing a rapid test for regions of debonds, lack of joining compound, or exceptionally thick or thin joints. Subsequently, these joined blocks were prepared with a saw cut for fracture testing as described below. Although detailed analysis of the joint signal - joint characteristic correlation was again not possible due to the limited number of joints produced, several main features were found in some specimens that could be identified. These served to delineate the sensitivity and limitations of this technique.

Microfocus X-ray Experiments

Radiography offers the advantage of rapid imaging of certain internal microstructural features in materials such as inclusions and voids. However, it produces only a through-transmission total absorption image of the material that often lacks contrast since microstructural features present only small differences in a usually large absorption value. With this in mind, it was not clear whether or not radiography would be useful for inspection of thin joint regions such as are produced by joining ceramics. This part of the program consisted of a series of experiments using microfocus radiography to assess the sensitivity of x-ray absorption measurements for joint characterization. The small source size of the x-ray unit used for these experiments provided for magnifications of the joint region and higher lateral resolution than conventional instruments. Two ceramic joints [(29(KY/1) and 29(KY/126)] were studied in detail with the x-ray unit and ultrasonically scanned as described below.

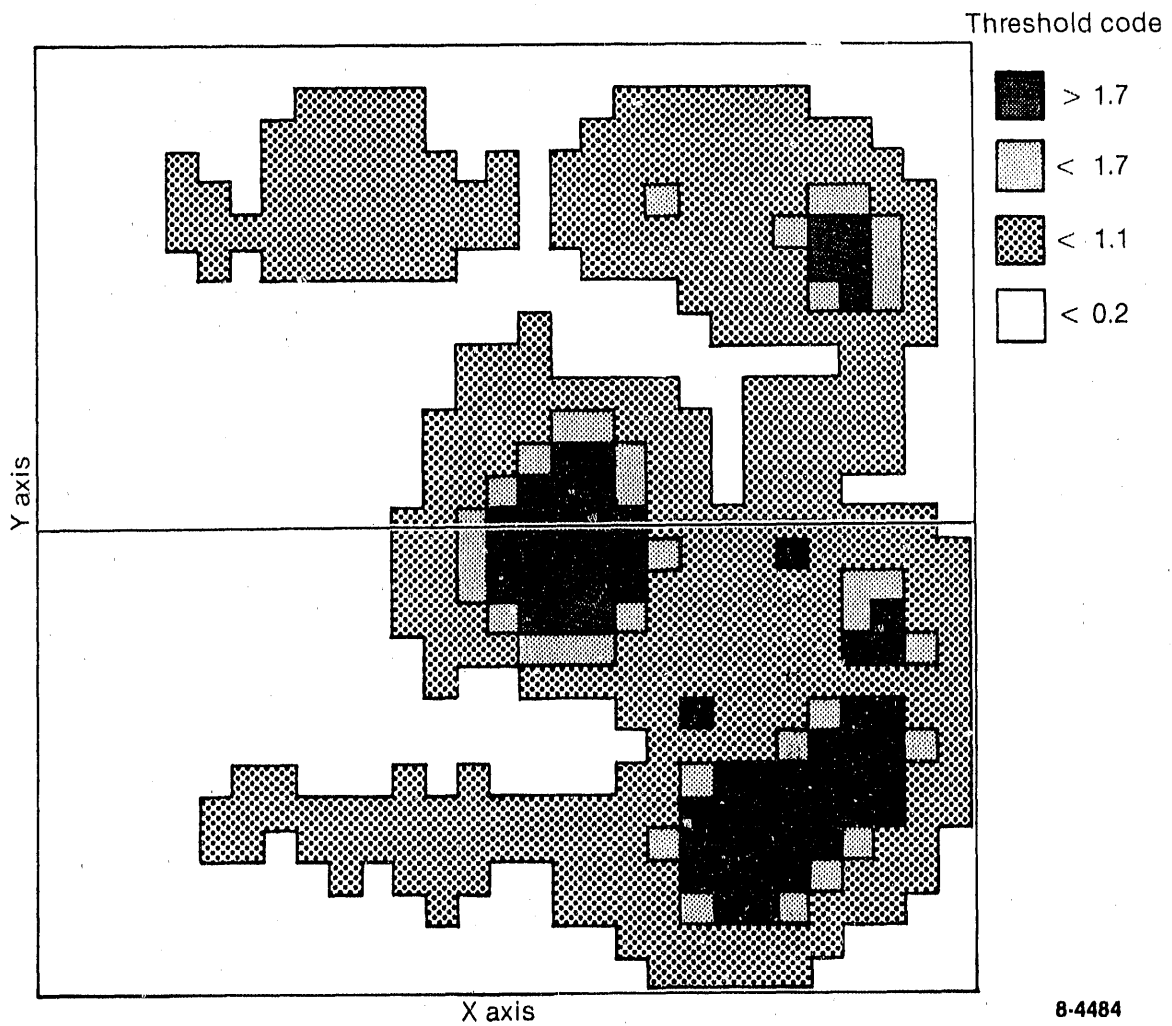
A distinct anomaly in the joint region was observed in the 29(KY/126) joint when projected at an angle with respect to the joint plane and was only faintly visible at normal incidence. The angular projection results helped to locate the anomaly in the joint plane and suggested that it was

of greater width than thickness. The 29(KY/1) joint showed no anomalies in the joint region, but there were indications near the outer surfaces of the sample. These results illustrated that the microfocus unit can be useful for inspecting the joint plane; however, considerable positioning capability must be used in order to take advantage of nonconventional off-axis projections through the joint plane. Significant increases in sensitivity and lateral resolution were observed by time averaging with film detection rather than using the real-time image intensifier technique.

Ultrasonic C-scans

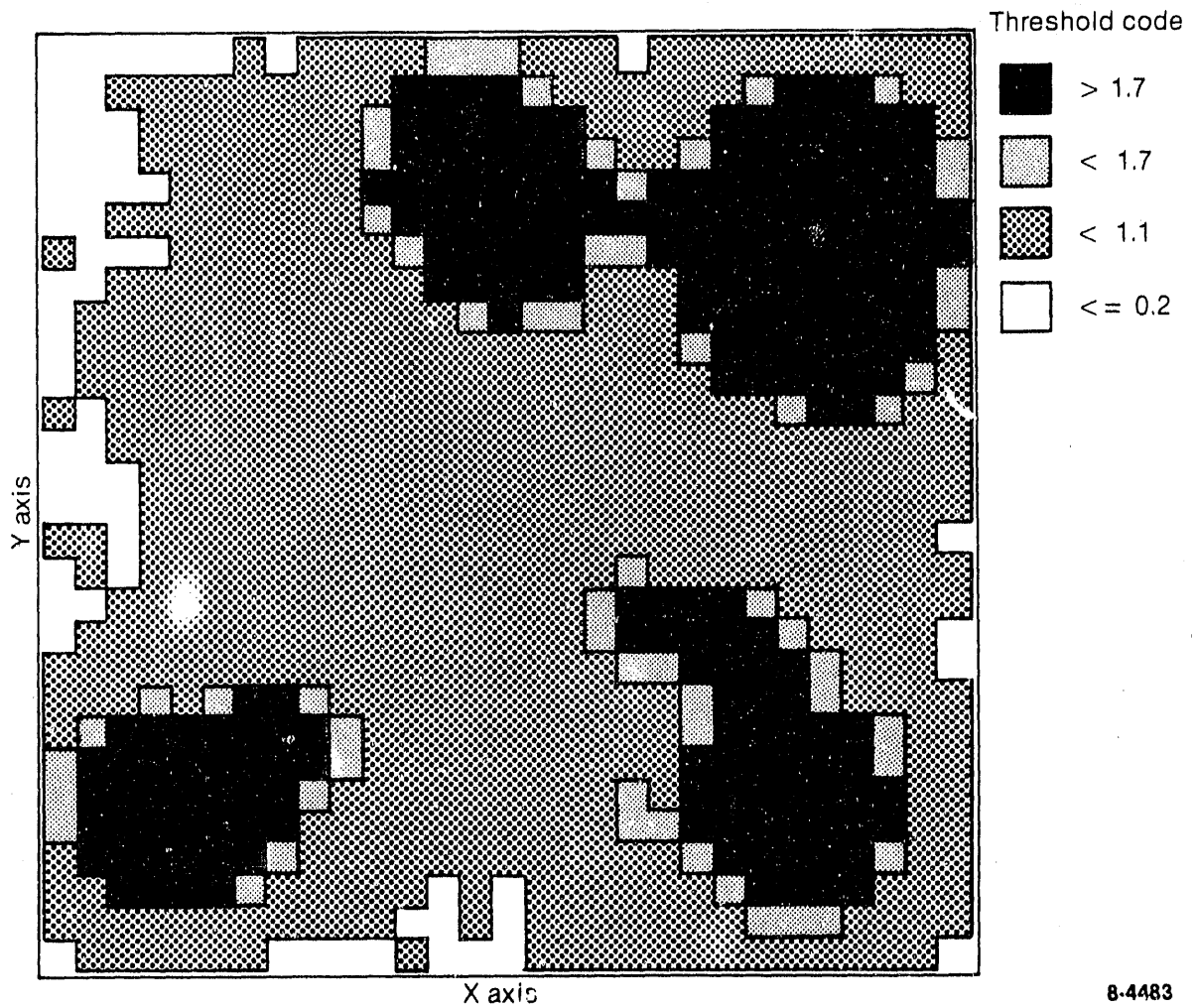
The joints were scanned, not only with the 80 MHz transducer, but with a 40 MHz transducer that was specially constructed without a delay line. A problem in the ultrasonic scanning performed to date has been the presence of extraneous echoes caused by the glass delay line attached to these transducers. The 40 MHz transducer was designed to eliminate this problem at the expense of fragility. The results were promising in that this transducer improved sensitivity with no extraneous echoes; however, it lacked the temporal resolution available from the higher frequency transducer with the delay line and was more sensitive to external electromagnetic interference because of insufficient shielding. Both ultrasonic scans recorded the same features. As an example of the detection sensitivity for an imbedded inclusion, the C-scan results of scanning two joints are shown in Figure 10, 29(KY/126) and Figure 11, 29(KY/1). The C-scans show a well defined scatterer in the joint plane for 29(KY/126) and no scatterer for 29(KY/1) away from the edge region. Particularly, Figure 11 is typical of many of the scan results, where the scattered signals near the edge come mainly from incomplete filling of the joint interface with the glassy material. However, Figure 10 shows a large reflection from the central region of the joint plane. This signal is more than one order of magnitude greater than the system noise level and was found to be from a glass filled flaw in the joint plane. Figure 12 shows a micrograph of this flaw section, which measures about 50 x 200 μm . The lateral spread shown in Figure 10 is due to the aperture size of the transducer used (about 3 mm).

Both radiography and ultrasonics characterized these two joints in a similar manner.



8-4484

Figure 10. C-scan of the joint reflection signal energy from 29(KY/126) joint, performed with an 80 MHz ($75 \mu\text{m}$ wavelength), 0.125-in. (3.2-mm) transducer. The central reflection is due to a $200 \times 50 \mu\text{m}$ glass filled flaw in the joint plane (see Figure 12).



8-4483

Figure 11. C-scan of the joint reflection signal energy from 29(KY/1) joint, performed with an 80 MHz (75 μm wavelength), 0.125-in. (3.2-mm) transducer. This joint was typical in that reflections came mainly from the outer edges where joining compound was missing.

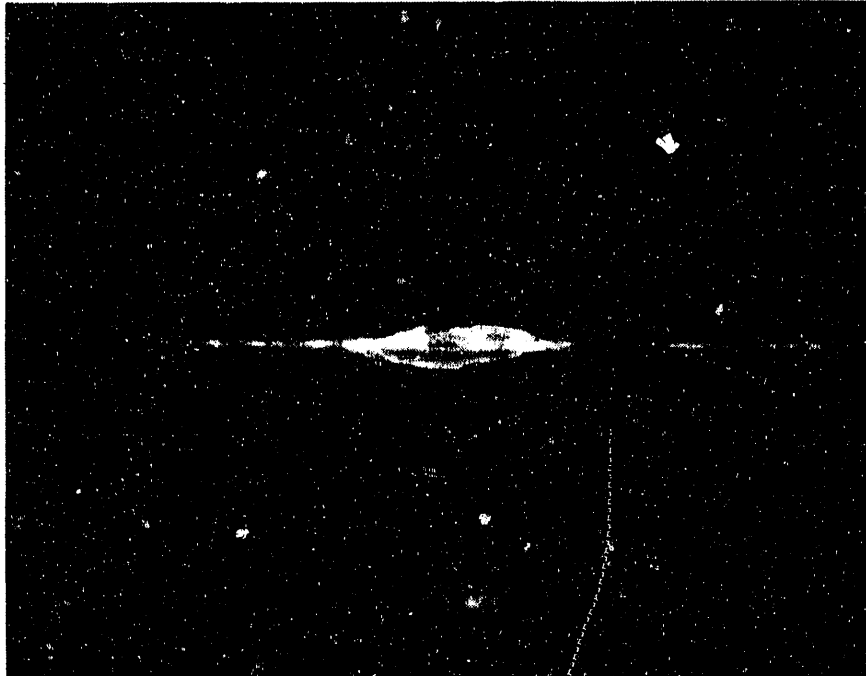


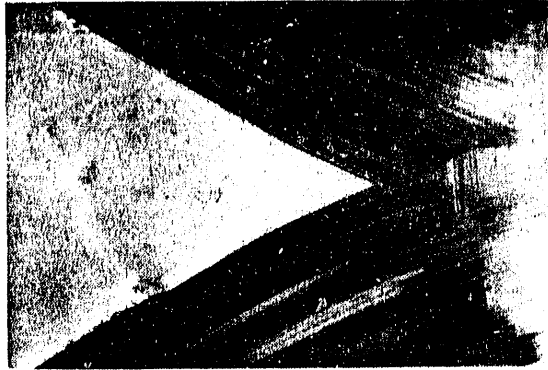
Figure 12. Micrograph of the detected flaw in joint 29(KY/126). The flaw appears to be glass filled and about 200 x 50 μm in size. Magnification is 100X.

CERAMIC HIPPED JOINTS - FRACTURE TESTS

Vee-Cuts

Specimens measuring 19 x 19 x 24 mm and 13 x 19 x 5 mm were fracture tested to measure the modulus of rupture for these HIPped joints. The results of ultrasonic scans were particularly useful in that regions of varying degrees of bonding were readily identified and judgments could be made as to the utility and exact nature of fracture testing needed for each joint before beginning the costly preparation of joint specimens. Some of the results of the joint imaging for fracture testing of the smaller joints are shown in Figure 13. As before, the figures display the value of the joint reflection signal energy obtained by scanning laterally over the specimen surface with the joint plane parallel to the specimen surface and 1-mm spacing between measurement points. Generally, the lighter colors shown indicate larger signal energies. Figure 13 shows the joint 25(KY/1) for a specimen made of Kyon ceramic bonded with glass by HIPping. The left side of the figure shows signals much smaller than the right. Model calculations of the reflection signal energy from a plane joint indicate that the large signals should be observed for thick joints and from regions of less glass bonding material, as with a void or high porosity region.

This specimen was subsequently prepared for fracture testing by sawing a slit along the joint, producing a "vee" as shown in the photograph of Figure 13. The specimen was then fractured by expanding this slit; the vee tip initiates the resulting crack. The amount of force necessary to split the specimen is a measure of the fracture toughness of the joint region. A distinct interruption in the fracture is seen to the left of the tip in the photograph which roughly correlates with the region where the joint reflection signal decreases as shown in the ultrasonic scan. Close examination shows that the fracture begins in the joint at the tip of the vee and then proceeds along the joint until it jumps into the lower ceramic block. This indicates that to the left of the break region the joint is stronger than the host ceramic material. The decrease in the ultrasonic signal energy indicates that this region is also where the joint is thinnest, assuming there are no voids in the joint region. Apparently, thinner joints are stronger, which may indicate more diffusion of the glass into the host ceramic and tighter bonding.



← Crack direction

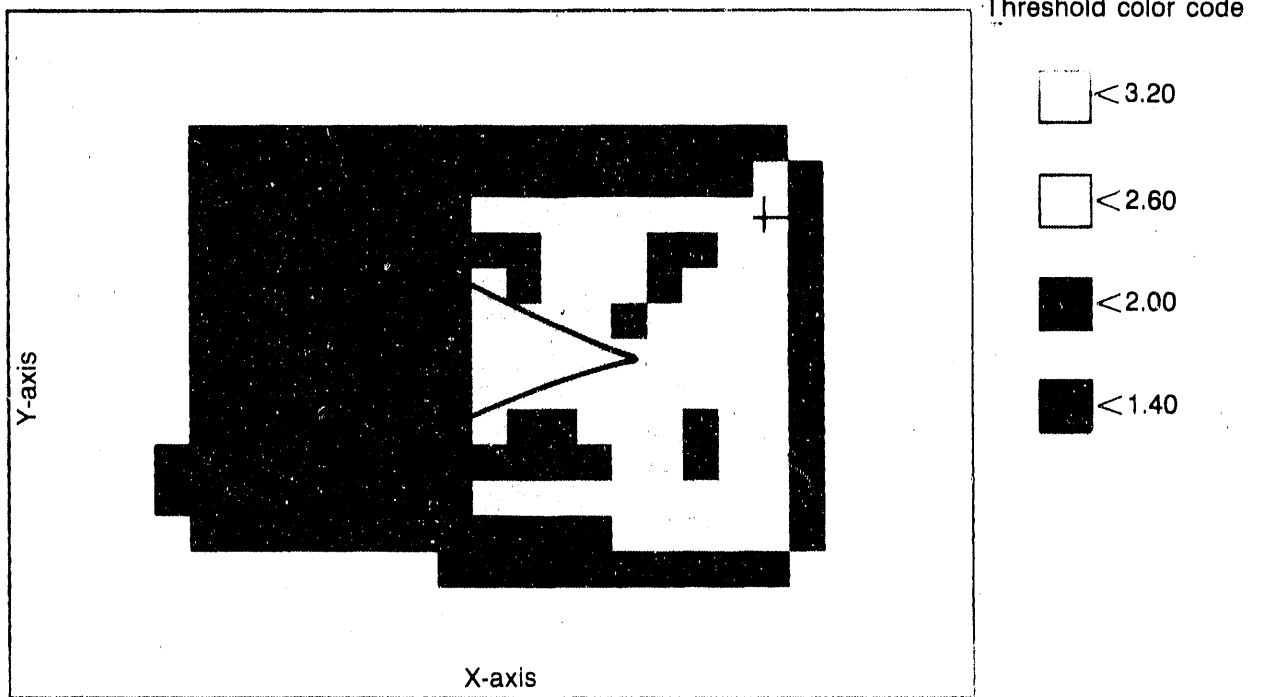
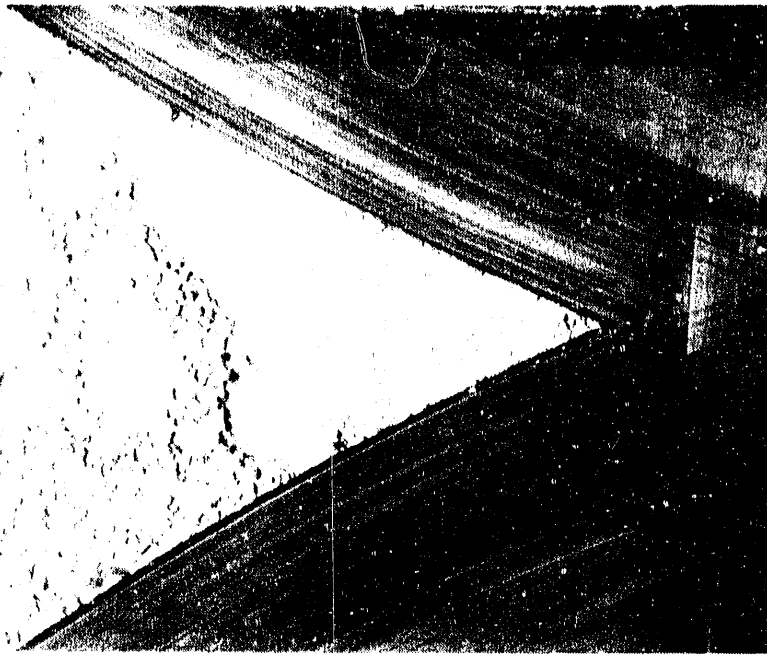


Figure 13. Plot of the joint reflection signal energies obtained by scanning before fracture testing for a HIPped Kyon/glass/Kyon joint 25(Ky/1). The "vee" indicates the joint region left after sawing a slit along the joint. The photograph above shows the crack surface after fracture to the same scale as the plot.

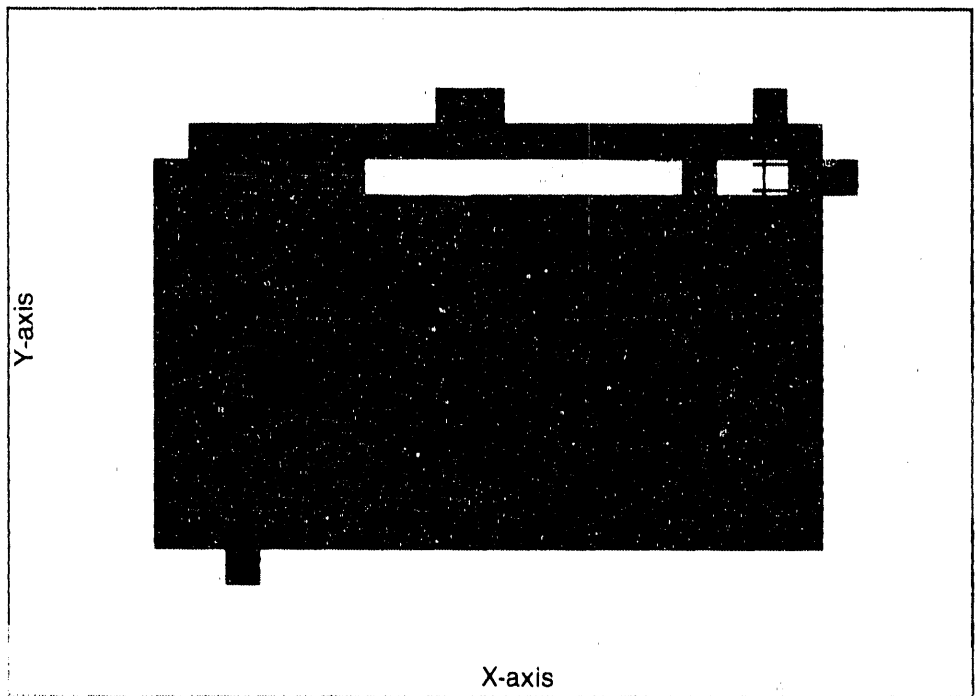
Figure 14 shows a scan from joint 20(NC/1), which was very uniform and consistently yielded small joint reflection signals. The photograph shows an enlarged view of the fracture, which was observed to jump repeatedly from the upper to the lower ceramic host material as it progressed along the joint. This behavior again indicates that the joint was as strong or stronger than the host material. From these results, it appears that ultrasonic measurements can reveal joint plane features that correlate with fracture toughness. More detailed examination is needed to determine exactly which joint characteristics (e.g., thickness or composition) are related to fracture toughness.

Modulus of Rupture Bars

The large joint specimens were cut along the long direction into 16 parts for modulus of rupture (MOR) measurements as shown in Figure 7. These cut specimens were used to perform tests at a variety of temperatures. This additional parameter, in conjunction with the fact that most joints had several unusable regions due to incomplete spreading of the joint compound, led to a severe limitation in the number of joints with a given set of characteristics that could be analyzed for detailed ultrasonic comparison. Consequently, at present, rather low statistics exist for the fracture toughness correlations and are not considered complete enough to be included in this report. The joint used for the thickness comparison contained four regions with different thicknesses, which were MOR tested at room temperature and at 1000°C. The room temperature results showed a slight monotonically decreasing modulus as the joint thickness increased. This may not be significant, however, as the statistical spread in this type of measurement is larger than the deviation observed. On the other hand, a significant change in the modulus of rupture was seen for the four sections tested at the higher temperature. The data are not understood at present and must be repeated to provide sufficient statistics for meaningful conclusions.



← Crack direction →



Threshold color code


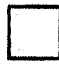


-  < 3.20
-  < 2.60
-  < 2.00
-  < 1.40

Figure 14. Plot of the joint reflection signal energies obtained by scanning before fracture testing for a HIPped NC/glass/NC joint 20(NC/1). The "vee" indicates the joint region left after sawing a slit along the joint. The photograph above shows the crack surface after fracture to an enlarged scale.

CONCLUSIONS

Research was performed to determine the feasibility of using reflected ultrasonic signal energy as a probe for determining important joint features. It is concluded that this form of ultrasonic testing is very applicable, having both qualitative and quantitative potential. Qualitatively, it is ideal for locating and assessing inclusions, voids, and regions of thin or thick joining compound throughout the joint plane by the C-scan method. Quantitatively, the value of the reflected signal energy can be used to measure joint thickness, given other controlled parameters. The results suggest that for a given range of thicknesses, measurement of the joint energy with broadband transducers with different center frequencies could provide a means of determining both the joint thickness and joint/host acoustic impedance mismatch. Joint thickness is potentially a critical feature in determining the fracture toughness of the joint itself. Further progress in this area will necessitate a detailed study with many joints produced with well characterized joint interfaces in order to obtain the correct statistics for verifying correlations between the joint features and the ultrasonic scans.

REFERENCES

1. K. L. Telschow et al., "Nondestructive Evaluation of Ceramic and RSA Joints and Materials," Strategic and Critical Materials Program Annual Report, May 1984 - 1987, Bureau of Mines Contract No. J0134035.
2. D. Coon et al., "Joining of Silicon Nitride-Based Ceramics," Strategic and Critical Materials Program Annual Report, May 1984 - 1987, Bureau of Mines Contract No. J0134035.

APPENDIX A

DERIVATION OF THE JOINT REFLECTION SIGNAL ENERGY: PLANE WAVE ANALYSIS

APPENDIX A

DERIVATION OF THE JOINT REFLECTION SIGNAL ENERGY: PLANE WAVE ANALYSIS

For this calculation, the ceramic surfaces and the joint plane are assumed to be flat and parallel. The composite ceramic component is submerged in water as the ultrasonic couplant. Let an initial plane wave of spectral amplitude $G(\omega)$ impinge normally on the ceramic surface from a water couplant medium. The first reflected wave is the front surface reflection

$$F(\omega) = r_{WC} G(\omega),$$

where r_{WC} is the water/ceramic reflection coefficient. The next signal observed comes from the joint interface, which presents a total reflection coefficient of r_j , which is tabulated below.^{A-1} Thus, the joint signal amplitude is

$$J(\omega) = t_{CW} r_j t_{WC} G(\omega),$$

where the transmission coefficients are related by:

$t_{CW} t_{WC} = 1 - r_{WC}^2$. Finally, the back surface reflection off the ceramic/water interface on the other side of the joint is given by

$$B(\omega) = r_{CW} t_{CW} t_{WC} t_j^2 G(\omega),$$

where t_j is the total joint transmission coefficient. The reflection and transmission coefficients can be written in terms of the relevant material acoustic impedance, assuming isotropic materials as

$$\begin{aligned} r_{WC} &= (Z_C - Z_W)/(Z_C + Z_W) & t_{WC} &= 2Z_C/(Z_C + Z_W) \\ r_{CW} &= (Z_W - Z_C)/(Z_C + Z_W) & t_{CW} &= 2Z_W/(Z_C + Z_W) \end{aligned}$$

The joint reflection and transmission coefficients are given by the acoustic coefficients for propagation through a barrier:^{A-1}

$$r_j^2 = 1 - t_j^2 \quad t_j^2 = 1/[\cos^2(kl) + Q^2 \sin^2(kl)],$$

$$r_j^2 = (Q^2 - 1) \sin^2(kl) / [\cos^2(kl) + Q^2 \sin^2(kl)],$$

where $Q = (Z_j/Z_c + Z_c/Z_j)/2$ and $kl = \omega l/v$, with $\omega = 2\pi f$,
 v the longitudinal wave velocity in the joint material and l the joint
interface thickness. The joint reflection signal energy is given by:

$$JE(\omega) = (1 - r_{wc}^2)^2 |G(\omega)|^2 [(Q^2 - 1)/Q^2] / [1 + (1/Q^2) \cot^2(kl)].$$

The total joint signal energy is then the integral of this term over the
nonzero spectral components of the initial waveform and is dependent only on
the joint properties through the ratio of the joint thickness to the
ultrasonic wavelength (kl) and the impedance ratio (Q). It is to be noted
that $Q \geq 1$, and typical values are between 1 and 2. Most of the salient
features of the signal energy equation can be illustrated by making some
simplifying assumptions:

1. Let $|G(\omega)|^2 = 1$, for $\omega_0 - b < \omega < \omega_0 + b$, which
is a square frequency spectra with a bandwidth of $2b$.
2. Assume $1 < Q < 2$, which is typical for many materials, then the
integrand $[1 + (1/Q^2) \cot^2(kl)]^{-1}$ is approximately equal to
 $\sin^2(kl)$, which is exactly true for $Q = 1$ (see Figure A-1).

The integral for the joint reflection signal energy can now be evaluated in
closed form:

$$JE = (1 - r_{wc}^2)^2 [(Q^2 - 1)/Q^2] \int_{\omega_0 - b}^{\omega_0 + b} \sin^2(\omega l/v) d\omega$$

$$JE = (1 - r_{wc}^2)^2 [(Q^2 - 1)/Q^2] b [1 - (\cos\{2\omega_0 l/v\} \sin\{2bl/v\}) / (2bl/v)]$$

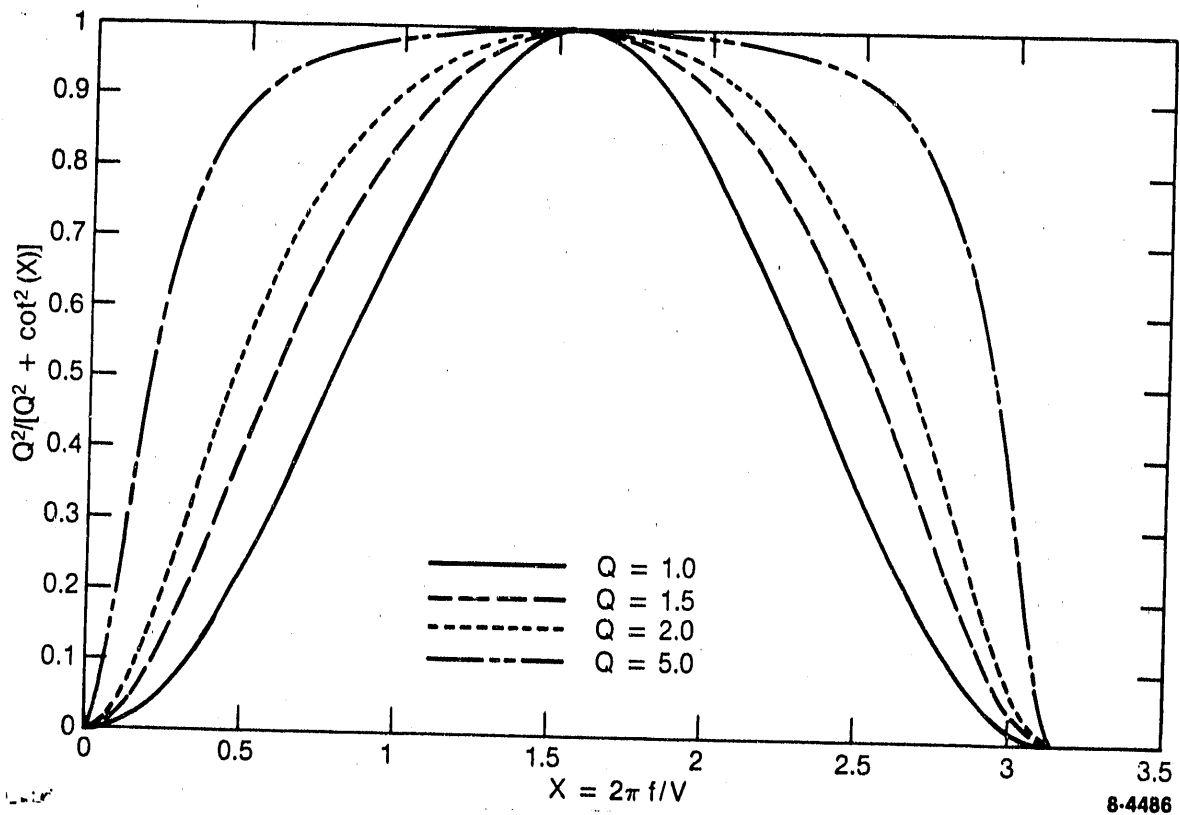


Figure A-1. Plot of the integrand function $[1 + (1/Q^2)\cot^2\{kl\}]^{-1}$ for various values of $Q = (Z_j/Z_c + Z_c/Z_j)/2$, with Z_j the bonding material impedance and Z_c the ceramic host impedance.

The thickness dependent part of this equation is plotted in Figure A-2. It will be noted from that figure that:

1. JE is proportional to $(Q^2 - 1)/Q^2$
2. JE is proportional to the transducer bandwidth $\{b\}$
3. JE is independent of thickness for $kl \gg \pi/2$ with wide bandwidth
4. JE is proportional to $(Q^2 - 1)/Q^2 (\tau^2/\lambda^2)$ for thin joints.

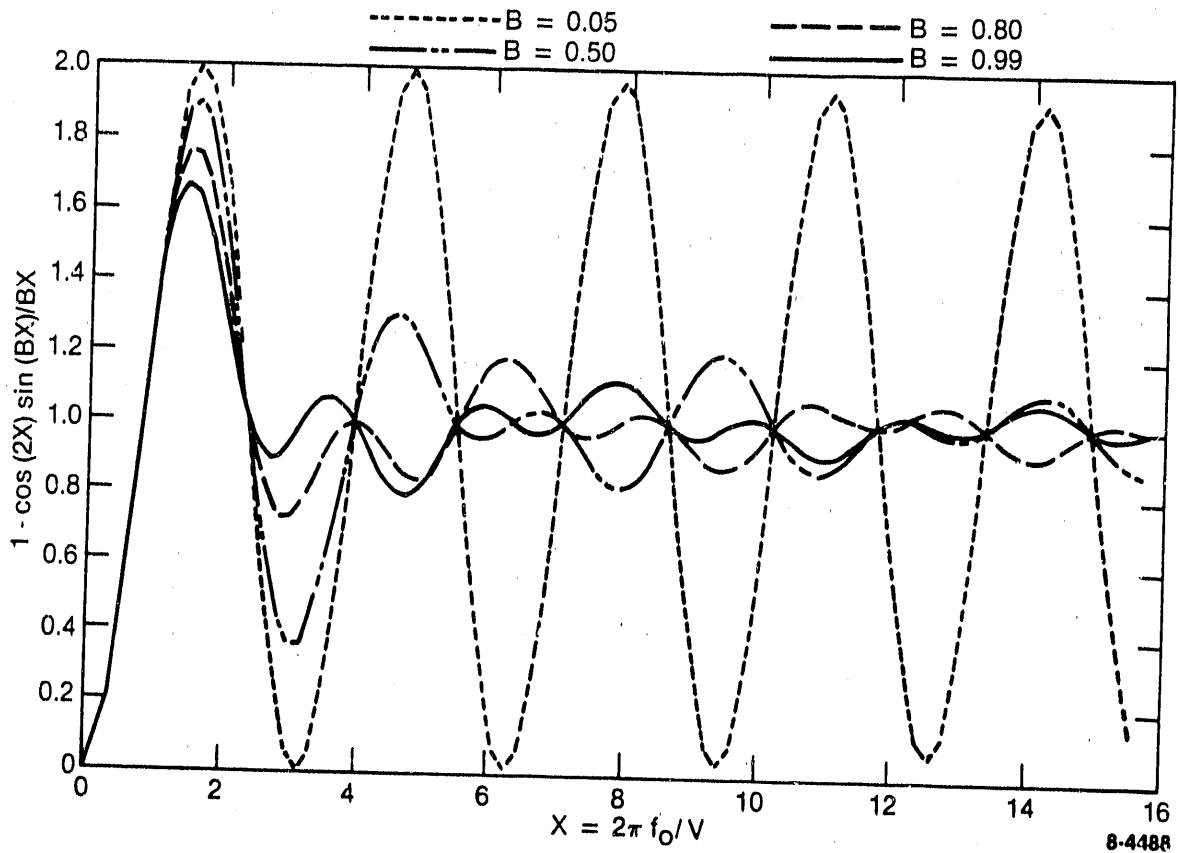


Figure A-2. Plot of the normalized joint signal energy for the simplified model (see Appendix A) for various values of the normalized bandwidth $B = 2b/\omega_0$.

REFERENCE

- A-1. S. Temkin, Elements of Acoustics, New York: John Wiley & Sons Publishing Co., 1981, pp. 103-111.

END

DATE FILMED

12 / 11 / 90

